

Cell Reports Medicine, Volume 4

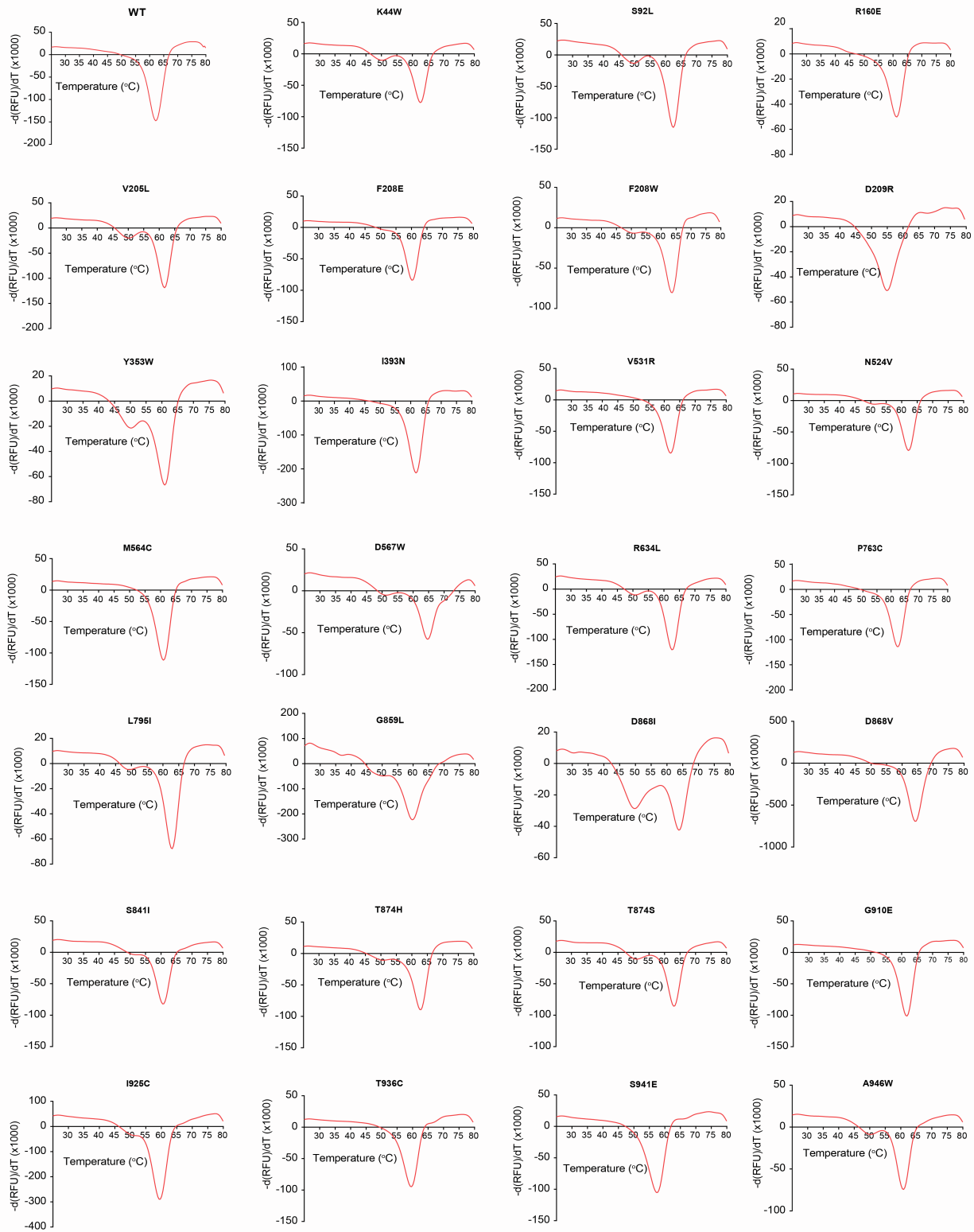
Supplemental information

Engineering highly thermostable Cas12b

via *de novo* structural analyses

for one-pot detection of nucleic acids

Long T. Nguyen, Santosh R. Rananaware, Lilia G. Yang, Nicolas C. Macaluso, Julio E. Ocana-Ortiz, Katelyn S. Meister, Brianna L.M. Pizzano, Luke Samuel W. Sandoval, Raymond C. Hautamaki, Zoe R. Fang, Sara M. Joseph, Grace M. Shoemaker, Dylan R. Carman, Liwei Chang, Noah R. Rakestraw, Jon F. Zachary, Sebastian Guerra, Alberto Perez, and Piyush K. Jain



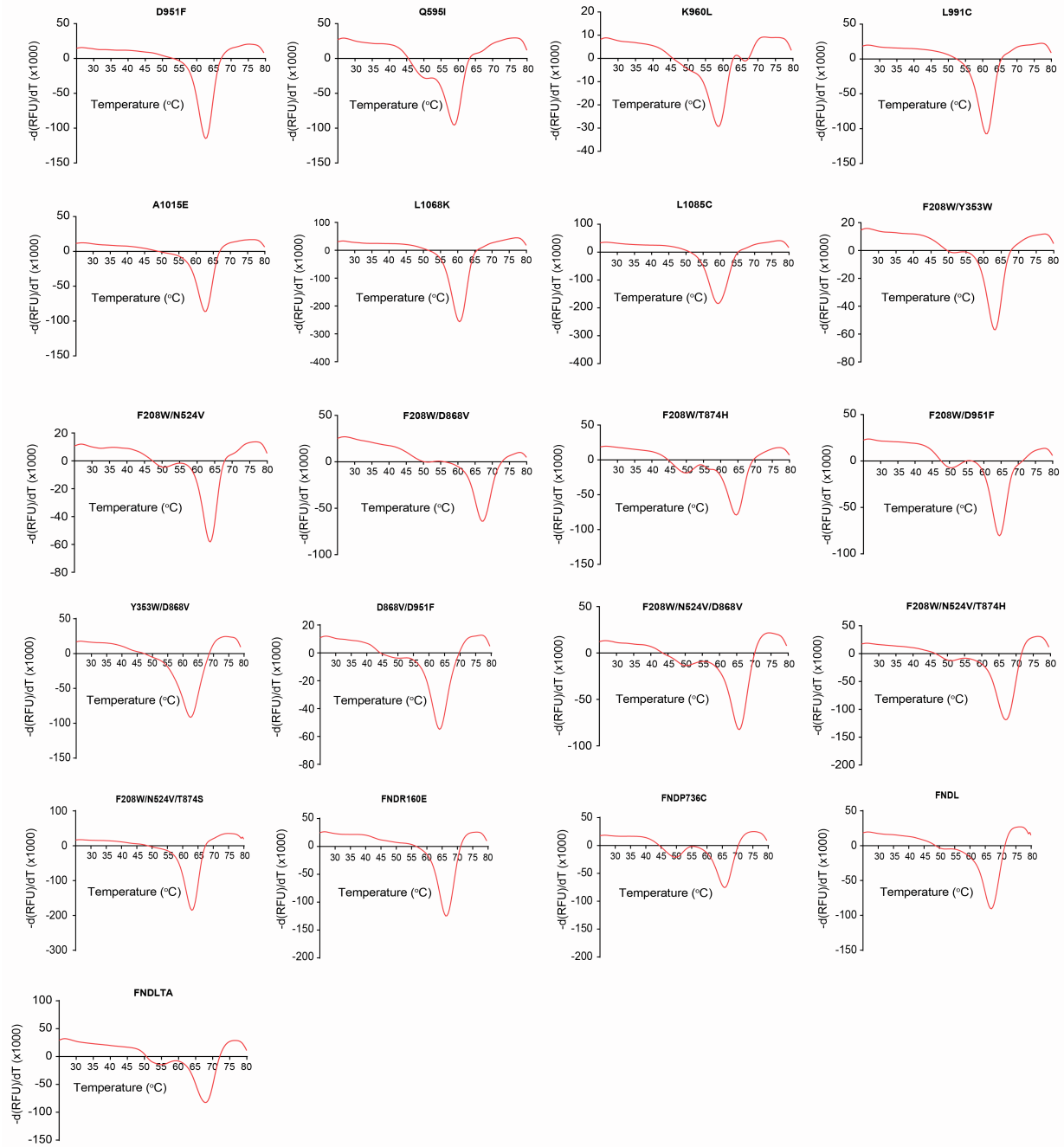
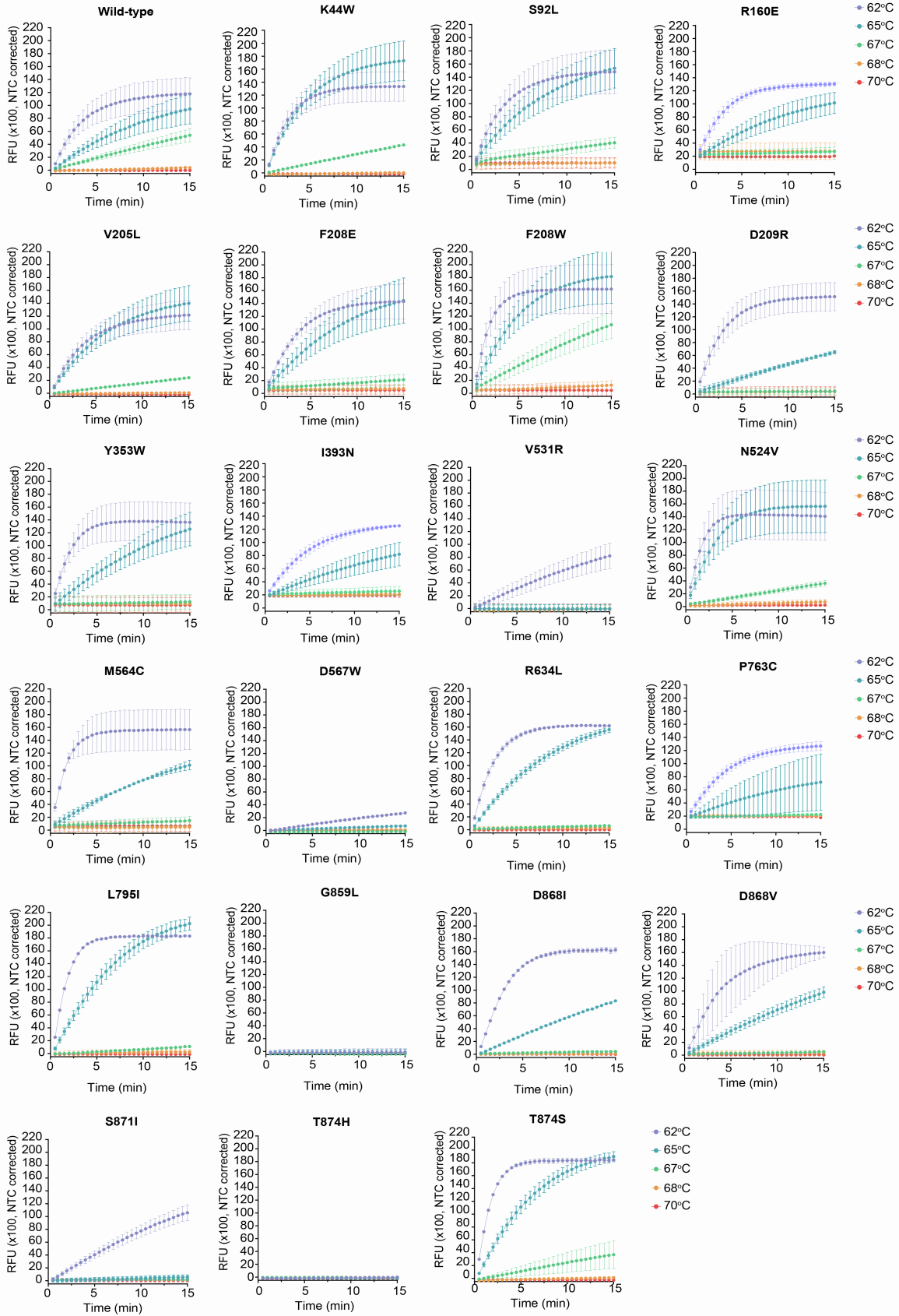


Figure S1. Differential Scanning Fluorometric Measurements of All BrCas12b Variants Used in the Study, Related to Figure 2 . The curve at each temperature point represents the average of fluorescence over 4 replicates ($n = 2$ technical replicates per experiment over two experiments). The melting point (T_m) was determined as a global minimum of the derivative curve.



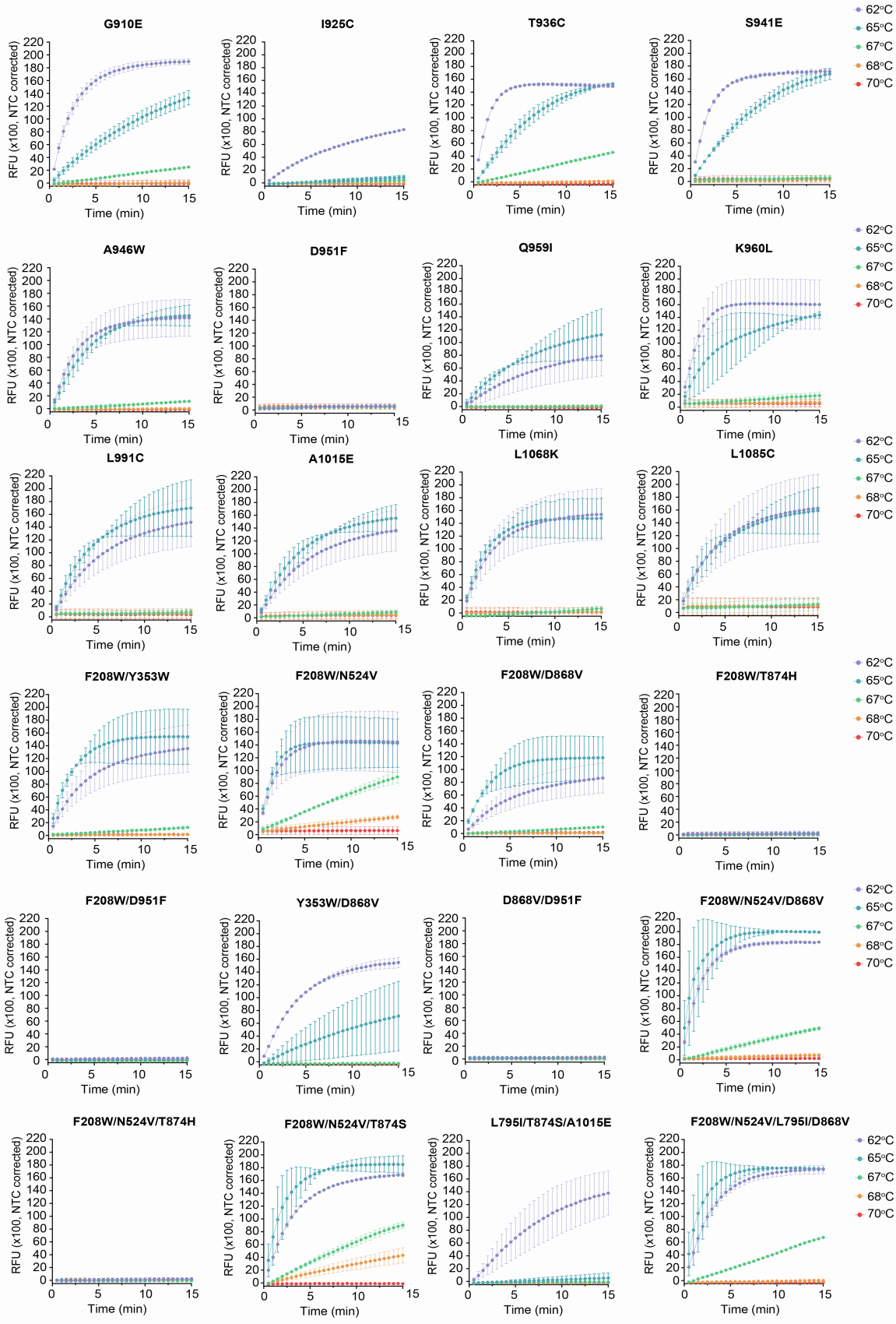


Figure S2. Time- and Temperature-dependent Trans-cleavage Activity of BrCas12b Variants Used in the Study, Related to Figure 2. The ribonucleoprotein complex and trans-cleavage reaction were incubated at 62°C, 65°C, 67°C, 68°C, and 70°C, respectively. Error bars represent mean \pm s.d., where n = 2 biological replicates.

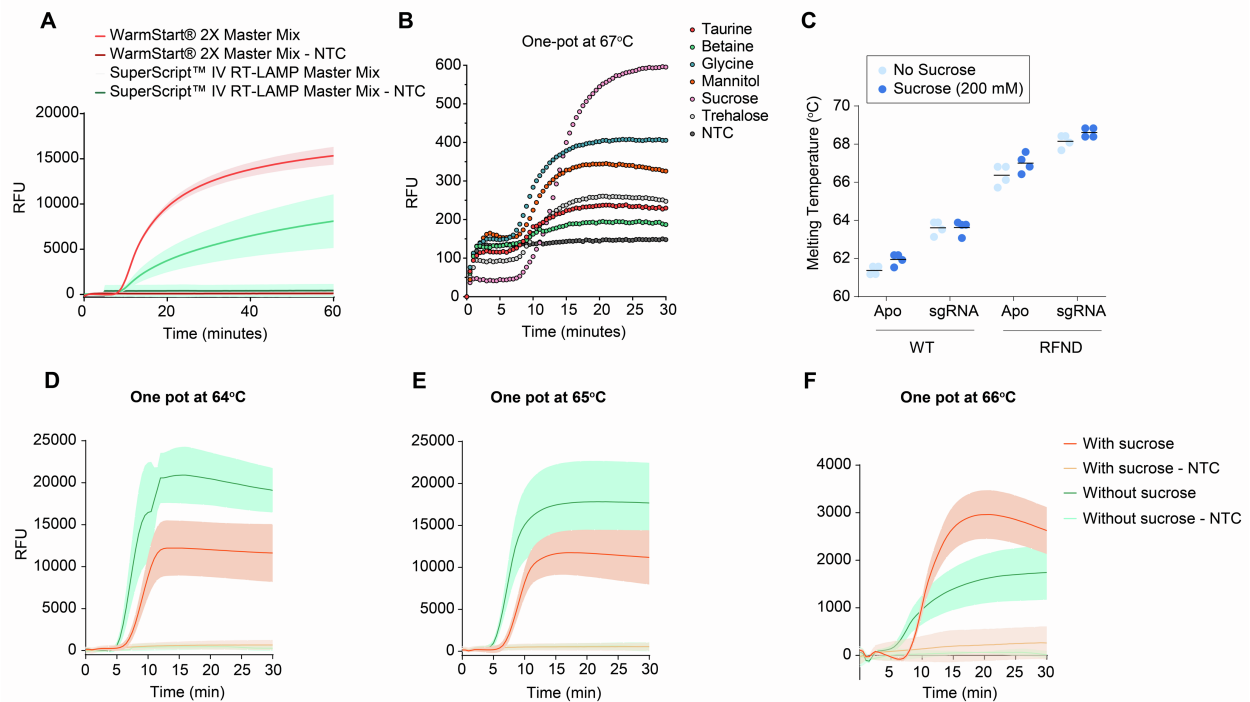


Figure S3. BrCas12b Detection Optimization, Related to Figure 4. (A) Compatibility of BrCas12b-based detection reaction with commercially available RT-LAMP master mixes. (B) Additive optimization of the one-pot reaction with additives for the FNDLTA variant. Additives were mixed to a final concentration of 50 mM, and the reaction was incubated isothermally at 67°C. Each data point represents an average of triplicates (n = 3 biological replicates). (C) Effects of sucrose on the thermostability of wild-type BrCas12b and the thermally improved RFND variant. Melting temperatures were determined from differential scanning fluorimetry (n = 2 technical replicates per experiment over two experiments). The melting point (T_m) was identified as a global minimum of the derivative RFU curve with respect to temperature. (D), (E), and (F) SPLENDID assay using RFND variant in the presence and absence of sucrose at 64°C, 65°C, 66°C, respectively. The SARS-CoV-2 genomic RNA input was 25,000 copies. The fluorescence measurements were taken at t = 30 minutes. Each curve represents the average of fluorescence signals. The shaded area represents standard deviation, n = 3.

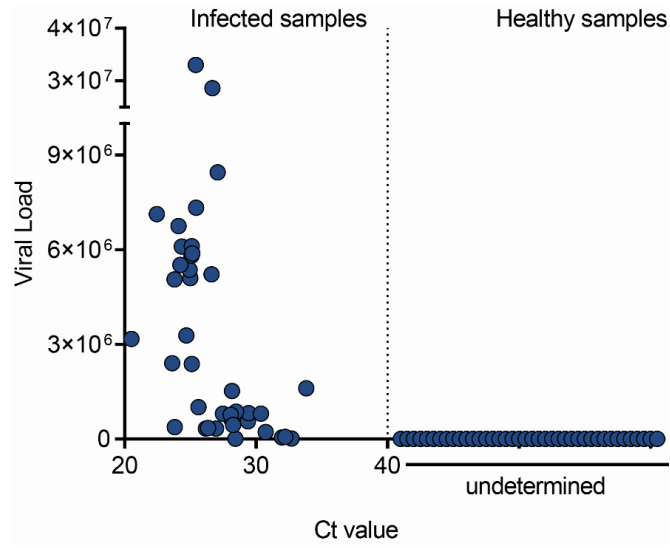


Figure S4. Correlation between In-house RT-qPCR and Clinically Validated Viral Loads for 80 HCV Patient Samples, Related to Figure 5.

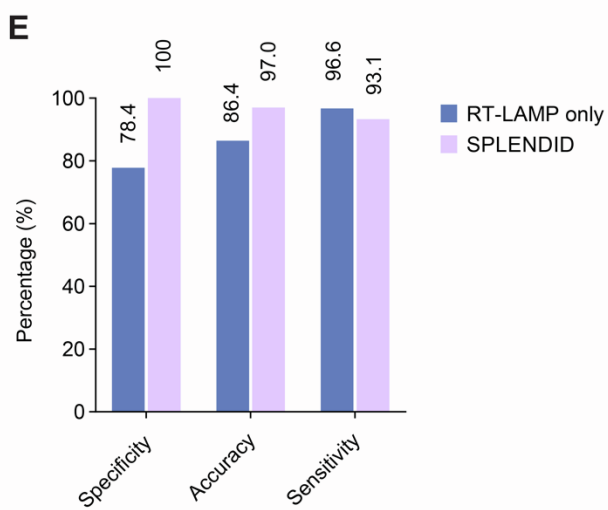
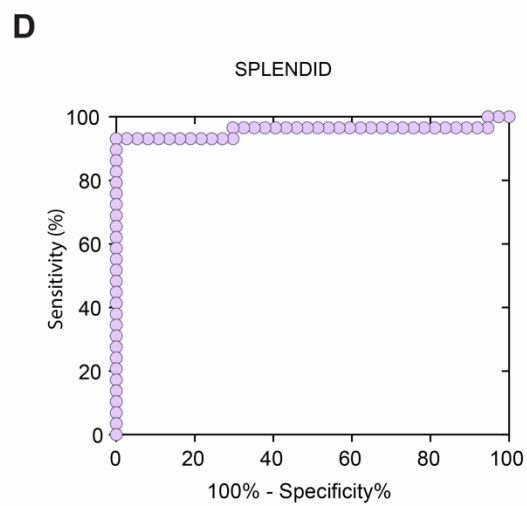
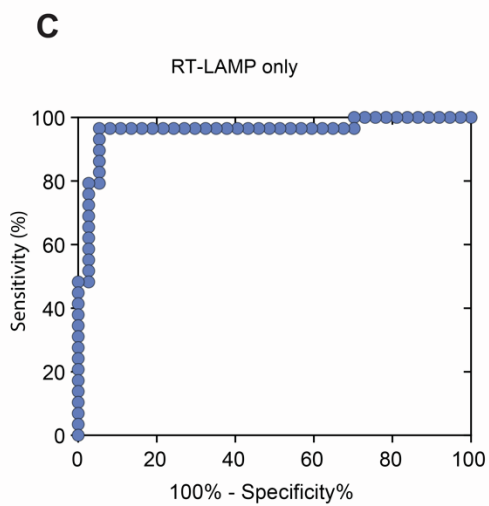
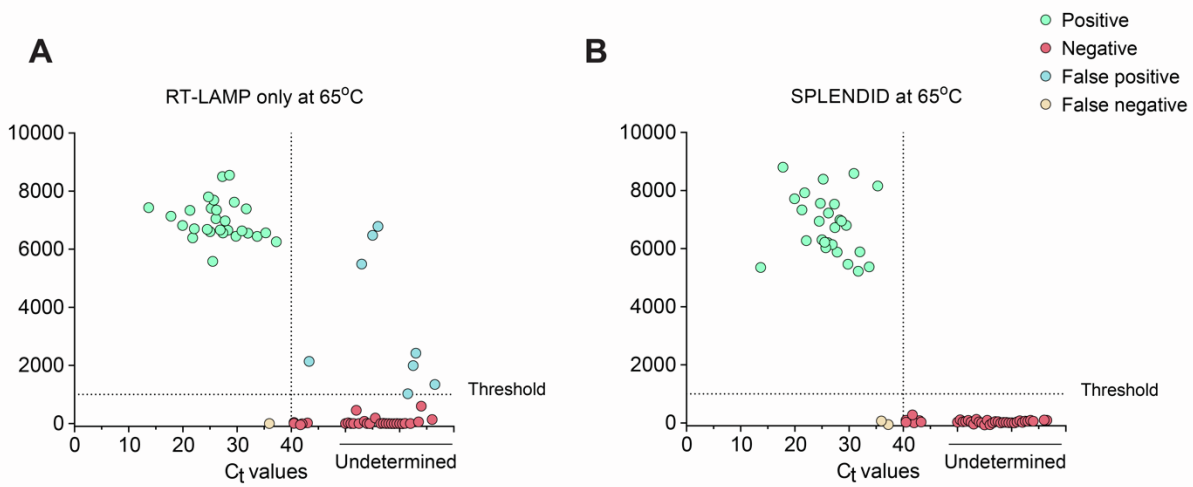


Figure S5. Clinical Validation of SPLENDID and RT-LAMP Only in SARS-CoV-2 Infected Samples, Related to Figure 5. (A) and (B) Fluorescence measurements of 66 SARS-CoV-2 clinical samples (29 negative and 37 positive samples) from the RT-LAMP only or SPLENDID assay, respectively. Signal readouts were taken at $t = 30$ minutes. (C) and (D) Receiver operating characteristic curve (ROC) at $t = 30$ minutes of RT-LAMP only and SPLENDID assays, respectively. (E) Summary of clinical validation of SPLENDID and RT-LAMP only in terms of sensitivity, specificity, and accuracy.

Table S1. Sequences Used in the Study, Related to Figure 1-5.

RT-LAMP primers

| Target | Name | Sequence |
|------------------------------------|------------|--|
| N gene of SARS-CoV-2 | N gene F3 | AACACAAGCTTTCGGCAG |
| | N gene B3 | GAAATTTGGATCTTTGTCATCC |
| | N gene FIP | TGCGGCCAATGTTTGTAAATCAGCCAA GGAA ATTTTGGGGAC |
| | N gene BIP | CGCATTGGCATGGAAGTCACCTTGTAT GGC ACCTGTGTAG |
| | N gene LF | TTCCTTGTCTGATTAGTTC |
| | N gene LB | ACCTTCGGGAACGTGGTT |
| 5' UTR of Hepatitis C ¹ | UTR F3 | CGGGAGAGCCATAGTGGT |
| | UTR B3 | WGGAWGTGTGCTCATGATGCACG |
| | UTR FIP | AAATCTCCAGGCATTGAGCGTTTTTTCGGGAACCGGTGAGTAC |
| | UTR BIP | CCGCRAGACYGCTAGCCGAGTTTTACCCTATCAGGCAGTACCAC |
| | UTR LF | TCGTCCYGGCRATTCCGG |
| | UTR LB | TAGTGTTGGGTCGCGAAAG |

Single-guide RNAs

| Target | Name | Sequence |
|-----------------------|--------------|---|
| N gene of SARS-CoV-2 | Br_sgN_CoV2 | GAAGGUGGUUAGCUACAGGCUGACCAGUGCAGUUGUGUCAUGUGCUACGG UGACCUAACACGUCACUCAGUCACAACGGCUAUCUAUUAUUUCCACUAACCA AAGUUAGUGGAAAUGUAGAUGGUUAGCACCGAAGAACGCUGAAGCGCUG |
| 5' UTR of Hepatitis C | Br_sgUTR_HCV | GAAGGUGGUUAGCUACAGGCUGACCAGUGCAGUUGUGUCAUGUGCUACGG UGACCUAACACGUCACUCAGUCACAACGGCUAUCUAUUAUUUCCACUAACCA AAGUUAGUGGAAAUGUAGAUGGUUAGCACUCCAAGAAAGGACCCGGUCG |

RT-qPCR primers²

| Target | Name | Sequence |
|-----------------------|---------------|--|
| 5' UTR of Hepatitis C | HCV_UTR_FOR | AGCGTCTAGCCATGGCGTT |
| | HCV_UTR_REV | GCAAGCACCTATCAGGCAGT |
| | HCV_UTR_Probe | /56-FAM/TCTGCGGAA/ZEN/CCGGTGAGT/3IABkFQ/ |

Reporters

| Target | Name | Sequence |
|-----------|------------|-------------------------|
| Universal | Reporter 1 | /5HEX/TTTTTTTT/3IABkFQ/ |
| | Reporter 2 | /5FAM/TTTTTTTT/3IABkFQ/ |

Protein sequences

| Name | Sequence |
|-----------|---|
| AapCas12b | MAVKSIVKLRLLDDMPEIRAGLWKLHKEVNAGVRYYTEWLSLLRQENLYR RSPNGDGEQECDKTAEECKAELLERLRARQVENGHRGPAGSDDELLQLA RQLYELLVPQAIGAKGDAQIARKFLSPLADKDAVGGGLGIKAGNKPRWV RMREAGEPGWEEKEKAETRKSADRTADVLRALADFLKPLMRVYTDSE MSSVEWKPLRKGQAVRTWDRDMFQQAIERMMSWESWNQRVGQEYAKL VEQKNRFEQKNFVQEHVHLVNQLQDMKEASPGLESKEQTAHYVTGR ALRGSQKVFQKLVGKLPDAPFDLYDAEIKNVQRRNTRRFQSHDLFAKLA |

| | |
|-----------------|--|
| | <p>PEYQALWREDASFLTRYAVYNSILRKLNHAKMFATFTLPDATAHPIWTRFD KLGGNLHQYTFLEFNEFGERRHAIRFHKLLKVENGVAREVDDVTPISMSE QLDNLLPRDPNEPIALYFRDYGAEQHFTGEFGGAKIQCRDQLAHMHRRR GARDVYLVNSVRVQSQSEARGERRPPYAAVFRLVGDNHRAFVHFDKLSD YLAEHPDDGKLGSEGLLSGLRVMSVDLGLRTSASISVFRVARKDELKPN KGRVPPFFPIKGNDNLVAVHERSQLLKLPGETESKDLRAIREERQRTLRL RTQLAYLRLLVRCGSEVDVGRRERSWAKLIEQPVDAANHMTDPDWREAFEN ELQKLKSLHGICSDKEWMDAVYESVRRVWRHMGKQVRDWRKDVRSGER PKIRGYAKDVVGGNSIEQIEYLERQYKFLKSWSFFGKVSQVIRAEKGSRF AITLREHIDHAKEDRLKKLADRIIMEALGYVYALDERGKWKVAKYPPCQLI LLEELSEYQFNDRPPSENNQLMQWVSHRGVFQELINQAQVHDLVGTMY AAFSSRFDARTGAPGIRCRVPARCTQEHNPFPWWLNKFVVEHTLDA CPLRADDLIPTGEGEIFVSPFSAEEGDFHQIHADLNAQNLLQQLWSDFDI SQIRLRCDWGEVDGELVLIPRLTGKRTADSYSNKVFYNTGTVYYERER KKRKVFVAQEKLSSEEAELLVEADEAREKSVLMDPSGIINRGNWTRQK EFWSMVNAQRIEGLVKQIRSRVPLQDSACENTGDI</p> |
| <p>BrCas12b</p> | <p>MPVRSFKVKLVTTRSGDAEHMLQLRRGLWKTHEIVNQGIAYMNLKALMR QEPYAGKSREVVRLLELLHSLRAQQKRNNWTGDAGTDDEILNLSRRLYELL VPSAIGEKGDAQMLSRKFLSPLVDPNSEGGKGTAKSGRKPWMMKREE GHPDWEAEREKDRAKKAADPTASILNDLEAFGLRPLFPLFTDEQKGIQWL PKQKRQFVRTFDRDMFQQALERMLSWESWNRRVAEEYQKLQAQRDELY AKYLADGGAWLEALQSFQREVELAEESFAAKSEYLITRRQIRGWKQVY EKWSQLPEHAAQEQFWQVADVQTSPLGAFGDPKVYQFLSQPEHHHIW RGYPNRLFHYSDYNGVRKKLQRARHDATFTLPDPVEHPLWIRFDARGGNI HDYEISQNGKQYQVTFSRLLWPENETWVERENVTAIGASQQLKRQIRLD GYADKKQKVRYRDYSSGIELTGVLGGAKIQFDRRHLRKASNRLADGETGP VYLVVVVVDIEPFLAMRNGRLQTPIGQVLQVNTKDWPKVTGYKPAELISWIQ NSPLAVGTGVNTIEAGMRVMSVDLGQRSAAAVSIFVMRQKPAEQETKLF YPIAVTGLYAVHRRSLLLRLPGEKISDEIEQQRKIRAHARSLVRYQIRLLADV LRLHTRGTAEQRRAKLDELLATLQTKQELDQKLWQTELEKLFDYIHEPAER WQQALVAAHRTLEPVIQAVRHWKSLRIDRKGLAGMSMWNIIEEETR KLLIAWSKHSRVPGEPNRLDKEETFAPQQLQHIQNVKDDRLKQMANLLVM TALGYKYDEAEKQWKEAYPACQMILFEDLSRYRFALDRPRENNRMLKW AHRIPRLVYLQGELFGIQVGDVYSAYTSRFHAKTGAPGIRCHALKEEDLQ PNSYVVKQLIKDGFIREDDTGSCLKPGQIVPWSGGELFVTLADRSGSRLAVI HADINAAQNLLQKRFWQQNTEIFRVPCVTTSGLIPAYDKMKKLFKGYFA KINQTDTSEVYVWEHSAKMKGKTPADPAEEGVFDESLEDEMEELEDSDQ EGYKTLFRDPSGFFWSSDRWLPQKEFWFWVKRRIEKKLREQLO</p> |

Table S2. Genotype Specific Sensitivity for HCV-patient Samples, Related to Figure 5

| Genotype | #samples | True Positive | False Negative | Sensitivity |
|-----------------|-----------------|----------------------|-----------------------|--------------------|
| GT1-(confirmed) | 34 | 31 | 3 | 91% |
| GT2-(confirmed) | 4 | 2 | 2 | 50% |
| GT3-(confirmed) | 2 | 0 | 2 | 0% |

Table S3. Summary of Detection Platforms, Related to Figure 5.

| | Target | Accuracy | Specificity | Sensitivity | Source |
|----------------|---------------|--------------------|--------------------|--------------------|--|
| RT-qPCR | SARS-CoV-2 | 95.8 | 91.3 | 99.5 | Banko <i>et al.</i> ³ |
| | HCV | 97% | 100% | NA | Chen <i>et al.</i> ⁴ , Zhang <i>et al.</i> ⁵ |
| STOP-Covid | SARS-CoV-2 | 95.8% | 98.5% | 93.1% | Joung <i>et al.</i> ⁶ |
| SPADE | SARS-CoV-2 | 96.7% | 99.4% | 92.8% | Nguyen <i>et al.</i> ⁷ |
| SHERLOCK | SARS-CoV-2 | NA | 100.0% | 96.0% | Patchesung <i>et al.</i> ⁸ |
| DETECTR | SARS-CoV-2 | 97.6% | 100.0% | 95.0% | Broughton <i>et al.</i> ⁹ |
| ENHANCE | SARS-CoV-2 | 95.0% | 96.8% | 96.8% | Nguyen <i>et al.</i> ¹⁰ |
| PMID: 35885430 | HCV | 97.0% | 100.0% | 96.0% | Kham-Kjing <i>et al.</i> ¹¹ |
| SPLENDID | HCV | 90.0% (overall) | 97.5% (overall) | 82.5% (overall) | This study |
| | | 94.6% (GT1) | 97.5% (overall) | 91.1% (GT1) | |
| | SARS-CoV-2 | 97.0% | 100.0% | 93.1% | |

References

1. Hongjaisee, S., Doungjinda, N., Khamduang, W., Carraway, T.S., Wipasa, J., Debes, J.D., and Supparatpinyo, K. (2021). Rapid visual detection of hepatitis C virus using a reverse transcription loop-mediated isothermal amplification assay. *Int J Infect Dis* 102, 440-445. 10.1016/j.ijid.2020.10.082.
2. Zauli, D.A., Menezes, C.L., Oliveira, C.L., Mateo, E.C., and Ferreira, A.C. (2016). In-house quantitative real-time PCR for the diagnosis of hepatitis B virus and hepatitis C virus infections. *Braz J Microbiol* 47, 987-992. 10.1016/j.bjm.2016.07.008.
3. Banko, A., Petrovic, G., Miljanovic, D., Loncar, A., Vukcevic, M., Despot, D., and Cirkovic, A. (2021). Comparison and Sensitivity Evaluation of Three Different Commercial Real-Time Quantitative PCR Kits for SARS-CoV-2 Detection. *Viruses-Basel* 13. ARTN 1321 10.3390/v13071321.
4. Chen, L.D., Li, W.L., Zhang, K., Zhang, R., Lu, T., Hao, M.J., Jia, T.T., Sun, Y., Lin, G.G., Wang, L.N., and Li, J.M. (2016). Hepatitis C Virus RNA Real-Time Quantitative RT-PCR Method Based on a New Primer Design Strategy. *J Mol Diagn* 18, 84-91. 10.1016/j.jmoldx.2015.07.009.
5. Zhang, E.Z., Bartels, D.J., Frantz, J.D., Seepersaud, S., Lippke, J.A., Shames, B., Zhou, Y., Lin, C., Kwong, A., and Kieffer, T.L. (2013). Development of a sensitive RT-PCR method for amplifying and sequencing near full-length HCV genotype 1 RNA from patient samples. *Virology* 453, 422-433. 10.1016/j.virol.2013.07.008.
6. Jung, J., Ladha, A., Saito, M., Kim, N.G., Woolley, A.E., Segel, M., Barretto, R.P.J., Ranu, A., Macrae, R.K., Faure, G., et al. (2020). Detection of SARS-CoV-2 with SHERLOCK One-Pot Testing. *N Engl J Med* 383, 1492-1494. 10.1056/NEJMc2026172.
7. Nguyen, L.T., Macaluso, N.C., Pizzano, B.L.M., Cash, M.N., Spacek, J., Karasek, J., Miller, M.R., Lednicky, J.A., Dinglasan, R.R., Salemi, M., and Jain, P.K. (2022). A thermostable Cas12b from *Brevibacillus* leverages one-pot discrimination of SARS-CoV-2 variants of concern. *Ebiomedicine* 77. ARTN 103926 10.1016/j.ebiom.2022.103926.
8. Patchsung, M., Jantarug, K., Pattama, A., Aphicho, K., Suraritdechachai, S., Meesawat, P., Sappakhaw, K., Leelahakorn, N., Ruenkam, T., Wongsatit, T., et al. (2020). Clinical validation of a Cas13-based assay for the detection of SARS-CoV-2 RNA. *Nat Biomed Eng* 4, 1140-1149. 10.1038/s41551-020-00603-x.
9. Broughton, J.P., Deng, X., Yu, G., Fasching, C.L., Servellita, V., Singh, J., Miao, X., Streithorst, J.A., Granados, A., Sotomayor-Gonzalez, A., et al. (2020). CRISPR-Cas12-based detection of SARS-CoV-2. *Nat Biotechnol* 38, 870-874. 10.1038/s41587-020-0513-4.
10. Nguyen, L.T., Rananaware, S.R., Pizzano, B.L.M., Stone, B.T., and Jain, P.K. (2022). Clinical validation of engineered CRISPR/Cas12a for rapid SARS-CoV-2 detection. *Commun Med (Lond)* 2, 7. 10.1038/s43856-021-00066-4.
11. Kham-Kjing, N., Ngo-Giang-Huong, N., Tragoolpua, K., Khamduang, W., and Hongjaisee, S. (2022). Highly Specific and Rapid Detection of Hepatitis C Virus Using RT-LAMP-Coupled CRISPR-Cas12 Assay. *Diagnostics (Basel)* 12. 10.3390/diagnostics12071524.